

Luminescent sol–gel thin films based on europium-substituted heteropolytungstates

Zheng Wang^{a,*}, Jun Wang^{b,c}, Hongjie Zhang^b

^a Faculty of Chemical and Material Science, Hubei University, Wuhan 430062, PR China

^b Key Laboratory of Rare Earth Chemistry and Physics, Changchun Institute of Applied Chemistry, Chinese Academy of Sciences, Changchun 130022, PR China

^c Centrum voor Oppervlaktechemie en Katalyse, Katholieke Universiteit Leuven, Leuven 3001, Belgium

Received 15 December 2003; received in revised form 4 March 2004; accepted 5 April 2004

Abstract

Polyester thin films containing europium-substituted heteropolytungstate were obtained on quartz plate by the sol–gel method. The films exhibited the characteristic emission bands of the europium ion. The red to orange intensity ratio (R:O) of Eu^{3+} in the films increased as compared to the corresponding heteropolytungstate solids. The fluorescence lifetime of europium is shorter in the thin film than in the heteropolytungstate solid. The results indicated that the formation of europium-substituted heteropolytungstate/polyester thin film has great effect on the luminescence of europium-substituted heteropolytungstate.

© 2004 Elsevier B.V. All rights reserved.

Keywords: Luminescence; Sol–gel; Europium; Polyoxometalate

1. Introduction

Rare earths have long been known for their characteristic luminescence properties. They have widely been used in cathodoluminescent display phosphor screens, liquid lasers, electroluminescent devices and as probe ions in biochemistry because of their high quantum yields of the emission, large Stokes shifts, long decay times and narrow emission bands [1–3]. Europium and terbium have attracted more attention because of their excellent luminescent characters. Europium complexes with β -diketones, aromatic carboxylic acids, crown-ethers and cryptates exhibit high color purity and strong fluorescent intensity due to the efficient energy transfer from organic ligands to the europium ion (the so-called antenna effect) through the triple state. In addition, ligands play an important role in protecting the europium ion from its environment (residual water or solvent molecules, etc.). This shielding effect considerably reduces the non-radiative de-activation process, which arises from coupling with the lattice vibrations and concentration quenching [4]. However, application of these organic complexes in optical devices is very limited due to their low thermal and mechanical resistance. Polyoxometalates are a

distinct class of multinuclear complexes with interesting optical, electric and magnetic properties. Rare earth-substituted polyoxometalates have been found exhibiting excellent luminescence properties and have been proved to be good candidates to fabricate hybrid organic/inorganic luminescent materials [5–7]. Recently, much attention has been directed to the sol–gel method in the preparation of optical materials containing rare earths because it offers the possibility of controlling the micro- and macrostructure of the optically transparent matrix [8]. However, conventional silica matrix tends to crack during the drying period. To improve the mechanical strength of the gels, we accommodate rare earth-substituted polyoxometalates into polymer matrix instead of silica matrix. In addition, polymer matrix provides different environment of rare earths through interaction with complexes.

In the present study, europium-substituted heteropolytungstates were incorporated into citric acid (CA)/polyethylene glycol (PEG) matrices by sol–gel method. Esterification of citric acid occurs readily in the presence of PEG at moderate temperature (100–150 °C). As citric acid has three carboxylic acid groups, branched polyesters may be obtained. During the process of polyesterification of CA and PEG, europium-substituted heteropolytungstates were entrapped in the gel polyester. The luminescent properties, lifetimes of thin films were studied with respect to the corresponding pure complexes.

* Corresponding author.

E-mail address: zwang805@yahoo.com.cn (Z. Wang).

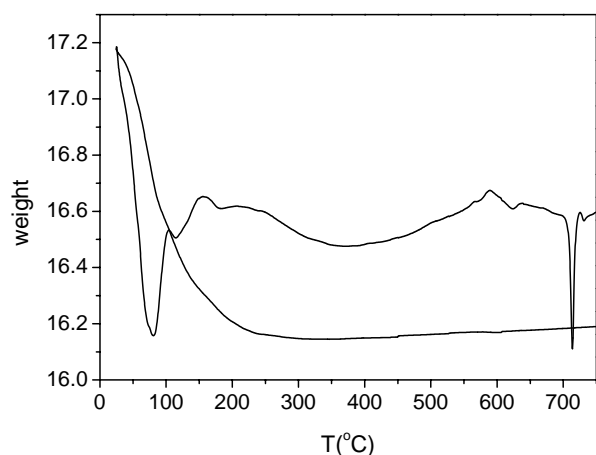


Fig. 1. TG-DTA figure of the EuSiW_{11} powder.

2. Experimental

2.1. Synthesis and characterization of

$K_m\text{Eu}(\text{XW}_{11}\text{O}_{39})_2 \cdot n\text{H}_2\text{O}$ ($X = \text{Si, Ge, B}$) complexes

$\text{K}_{13}\text{Eu}(\text{SiW}_{11}\text{O}_{39})_2 \cdot 28\text{H}_2\text{O}$ (EuSiW_{11}), $\text{K}_{13}\text{Eu}(\text{GeW}_{11}\text{O}_{39})_2 \cdot 25\text{H}_2\text{O}$ (EuGeW_{11}) and $\text{K}_{15}\text{Eu}(\text{BW}_{11}\text{O}_{39})_2 \cdot 22\text{H}_2\text{O}$ (EuBW_{11}) were prepared according to references [9,10]. The molecular formulas of the products were confirmed on the basis of elemental analysis, IR and TG-DTA analysis.

Fig. 1 represented the thermal decomposition of EuSiW_{11} . EuSiW_{11} decomposed in three consecutive steps. The first mass loss occurred in the temperature range of 25–95 °C with the loss of 4.5% of the material, the second mass loss took place in the temperature range of 97–147 °C with 1.5% loss, and the third mass loss took place in the temperature range of 150–280 °C with 1.0% loss. The DTA plot showed four distinct endothermic peaks, three of which at 80, 115 and 183 °C corresponded to the loss of water molecule, the other one at 714 °C corresponded to the melting of EuSiW_{11} . Fig. 2 showed the IR spectrum of EuSiW_{11} . The IR spectrum of EuSiW_{11} had four regions [11], which

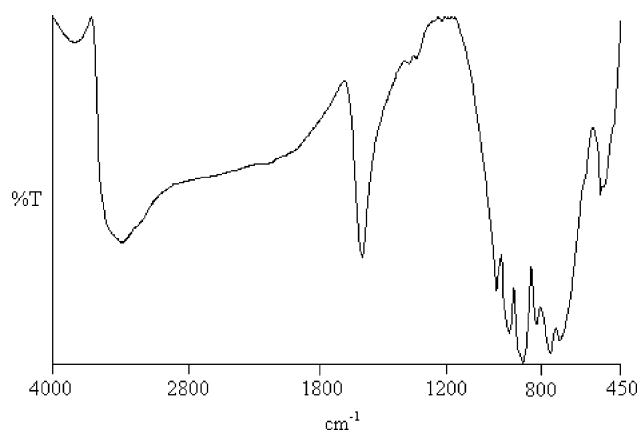


Fig. 2. IR spectra of the EuSiW_{11} powder.

corresponded to metal–oxygen oscillations including Si–O stretching (1008.6 cm^{-1}), W–O stretching (951.9 cm^{-1}), and W–O–W stretching ($900\text{--}600\text{ cm}^{-1}$).

2.2. Thin film preparation

Appropriate amounts of $\text{K}_m\text{Eu}(\text{XW}_{11}\text{O}_{39})_2 \cdot n\text{H}_2\text{O}$ (EuXW_{11}) ($X = \text{Si, Ge, B}$) were dissolved in the aqueous solution of citric acid and polyethylene glycol (molecular weight 10,000). The molar ratio of EuXW_{11} , citric acid and polyethylene glycol was 1:2:0.5. A little excess portion of polyethylene glycol was to guarantee the esterification of the three carboxylic acid groups of citric acid. The mixture was stirred for about 3 h at room temperature. A homogeneous transparent solution was obtained and it was dip-coated on a quartz plate. The coating was dried in a drying oven for 3 h at 150 °C and the resulting thin film was stored in a desiccator for further measurements.

2.3. Measurements

The TG-DTA measurements were made with a SDT2960 thermal analyzer. IR spectra were recorded on a Nicolet 170 spectrophotometer using KBr pellets. UV-vis spectra were recorded on a Tu-1901 spectrophotometer. Luminescence spectra were measured on a Spex FL-2T2 spectrophotometer using xenon lamp as excitation source. Luminescence lifetime of Eu^{3+} was recorded on a Spex 1934D-phosphorescence spectrophotometer.

3. Results and discussion

3.1. UV spectra

The UV spectra of $\text{K}_m\text{Eu}(\text{XW}_{11}\text{O}_{39})_2$ (EuXW_{11}) ($X = \text{Si, Ge, B}$) solutions and EuXW_{11} /polyester films are measured. Two major bands corresponded to the characteristic $\text{O} \rightarrow \text{W}$ transitions of heteropolytungstates are observed both in the spectra of EuXW_{11} solutions and in the spectra of EuXW_{11} /polyester films. Fig. 3 illuminates the UV spectra of the EuSiW_{11} solution and the EuSiW_{11} /polyester film. EuSiW_{11} solution shows characteristic absorption bands of EuSiW_{11} at 199 and 250 nm, which correspond to the $\text{O}_d \rightarrow \text{W}$ and $\text{O}_{b,c} \rightarrow \text{W}$ charge transitions, respectively. In the EuSiW_{11} /polyester film, characteristic absorption bands of EuSiW_{11} can be observed and the peaks are red shift to 202 nm ($\text{O}_d \rightarrow \text{W}$) and 255 nm ($\text{O}_{b,c} \rightarrow \text{W}$), respectively. From the facts above, we can conclude that EuSiW_{11} has been successfully incorporated in the polyester film. The same phenomena can be observed in the absorption spectra of $\text{K}_m\text{Eu}(\text{XW}_{11}\text{O}_{39})_2$ ($X = \text{Ge, B}$) and their polyester films. UV data of EuXW_{11} solution and EuXW_{11} /polyester films are listed in Table 1. Differences between the UV spectra of EuXW_{11} solution and EuXW_{11} /polyester films can be attributed to the interactions between EuXW_{11} and polyester

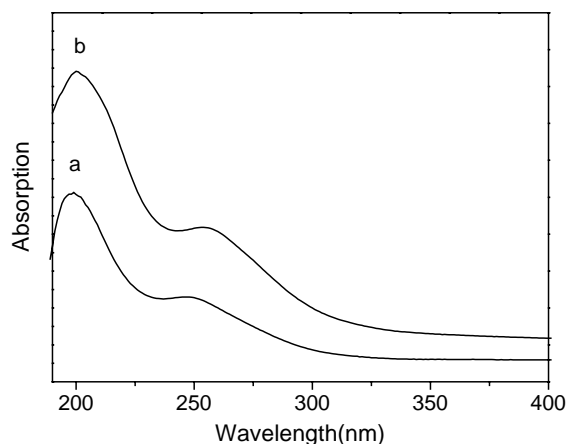


Fig. 3. UV spectra of the EuSiW_{11} solution (a) and the EuSiW_{11} /polyester film (b).

Table 1

UV data of EuXW_{11} solutions and EuXW_{11} /polyester films ($X = \text{Si, Ge, B}$)

	$\text{O}_d \rightarrow \text{W}$ transition	$\text{O}_{b,c} \rightarrow \text{W}$ transition
EuSiW_{11} solution	199	250
EuSiW_{11} /PE film	202	255
EuGeW_{11} solution	198	252
EuGeW_{11} /PE film	203	255
EuBW_{11} solution	197	250
EuBW_{11} /PE film	202	254

matrix, which influence the $\text{O} \rightarrow \text{W}$ charge transitions of europium-substituted heteropolytungstates.

3.2. Excitation and emission spectra of EuSiW_{11} /polyester film and EuSiW_{11} solid

Fig. 4 shows the excitation spectra of the EuSiW_{11} solid (solid line) and the EuSiW_{11} /polyester film (dash line). The excitation spectrum of the EuSiW_{11} solid consists of char-

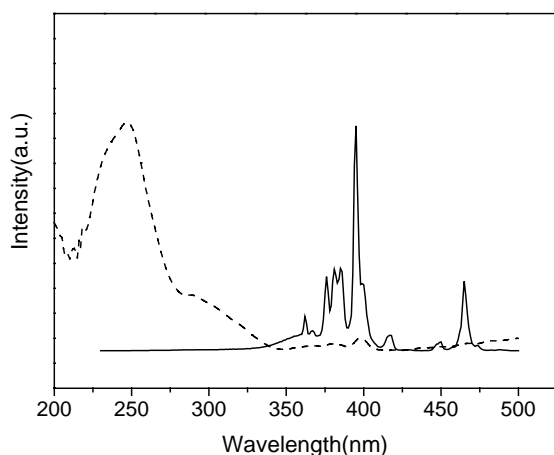


Fig. 4. Excitation spectra of the EuSiW_{11} solid (solid line) and the EuSiW_{11} /polyester film (dash line).

acteristic peaks of Eu^{3+} at 362, 376, 381, 385, 395, 417 and 465 nm, which correspond to $^7\text{F}_0 \rightarrow ^5\text{D}_4$, $^7\text{F}_0 \rightarrow ^5\text{G}_4$, $^7\text{F}_0 \rightarrow ^5\text{G}_3$, $^7\text{F}_0 \rightarrow ^5\text{G}_2$, $^7\text{F}_0 \rightarrow ^5\text{L}_6$, $^7\text{F}_0 \rightarrow ^5\text{D}_3$ and $^7\text{F}_0 \rightarrow ^5\text{D}_2$ transitions, respectively. Nevertheless, the excitation spectrum of the EuSiW_{11} /polyester film differs greatly from that of the EuSiW_{11} solid. The EuSiW_{11} /polyester film shows a strong wide band from 210 to 270 nm with a maximum peak at 250 nm and some weak characteristic peaks of Eu^{3+} . The wide band is assigned to ligand-to-metal charge transfer (LMCT) band, which has a close relationship with the luminescence of the complex. The difference between the spectrum of the EuSiW_{11} solid and the EuSiW_{11} /polyester film indicates that the energy transfer process is different in different states of the complex. In the excitation spectrum of the EuSiW_{11} solid, there are only sharp excited lines of Eu^{3+} and no charge transfer band could be found. This shows that the luminescence of the EuSiW_{11} solid was mainly contributed by the excitation of Eu^{3+} . This kind of excitation could hardly result in efficient luminescence of the complex [12]. In EuSiW_{11} , Eu^{3+} is coordinated by two SiW_{11} groups through eight oxygen atoms forming an Archimedean antiprism. The extent of the delocalization of the d^1 electron in SiW_{11} ligand is great at room temperature. As a result, the energy excited into SiW_{11} can hardly transfer to Eu^{3+} effectively, but falls back to the ground state by the non-radiative transition. That is why we cannot observe the LMCT band in the EuSiW_{11} solid. However, an intense LMCT band of EuSiW_{11} ($\lambda_{\text{max}} = 250$ nm) emerges in the EuSiW_{11} /polyester film, which indicates that the energy can be effectively transferred to Eu^{3+} in the EuSiW_{11} /polyester film. The formation of the EuSiW_{11} /polyester film reduces the delocalization of the d^1 electron in SiW_{11} ligand. The energy level of LMCT band of EuSiW_{11} differs from before the entrapment of EuSiW_{11} in polyester. Strengthened interaction between the energy level of Eu^{3+} and LMCT band of EuSiW_{11} makes possible the energy transfer from ligands to rare earths.

The emission spectra of the EuSiW_{11} solid (solid line) and the EuSiW_{11} /polyester film (dash line) excited at 395 and 250 nm, respectively, are shown in Fig. 5. Both of the solid and the film exhibit characteristic emission of Eu^{3+} ion, which originates from $^5\text{D}_0$ excited state of Eu^{3+} and terminates at $^7\text{F}_j$ ($j = 0-4$) ground state. It is obvious that the transitions correspond to $^5\text{D}_0 \rightarrow ^7\text{F}_1$ and $^5\text{D}_0 \rightarrow ^7\text{F}_2$ are much stronger than those correspond to $^5\text{D}_0 \rightarrow ^7\text{F}_j$ ($j = 0, 3, 4$). The $^5\text{D}_0 \rightarrow ^7\text{F}_1$ transition is a magnetic dipole transition and its intensity varies with the crystal field strength acting on Eu^{3+} ions. As to the $^5\text{D}_0 \rightarrow ^7\text{F}_2$ transition, it is an electric dipole transition and is extremely sensitive to chemical bonds in the vicinity of the Eu^{3+} ion. The possibility of $^5\text{D}_0 \rightarrow ^7\text{F}_2$ transition will increase drastically if the site symmetry of Eu^{3+} ion decreases. As a result, the intensity ratio of the $^5\text{D}_0 \rightarrow ^7\text{F}_2$ transition to $^5\text{D}_0 \rightarrow ^7\text{F}_1$ transition has been widely used as an indicator of Eu^{3+} site symmetry. In the EuSiW_{11} solid, the $^5\text{D}_0 \rightarrow ^7\text{F}_1$ and $^5\text{D}_0 \rightarrow ^7\text{F}_2$ transitions split into two peaks at 592, 594 nm

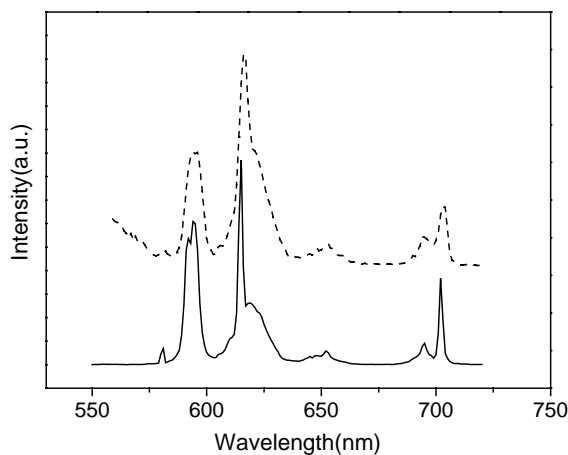


Fig. 5. Emission spectra of the EuSiW₁₁ solid (solid line) and the EuSiW₁₁/polyester film (dash line).

and 615, 619 nm, respectively. The emission peak at 581 nm corresponds to the $^5D_0 \rightarrow ^7F_0$ symmetric forbidden emission and the peak at 651 nm is due to the $^5D_0 \rightarrow ^7F_3$ transition. The splitting peaks at 694–701 nm can be assigned to the transition of $^5D_0 \rightarrow ^7F_4$. However, no splitting was observed in the transition of $^5D_0 \rightarrow ^7F_1$ and $^5D_0 \rightarrow ^7F_2$ in the EuSiW₁₁/polyester film. The relative intensity of the $^5D_0 \rightarrow ^7F_2$ transition to $^5D_0 \rightarrow ^7F_1$ transition increased after EuSiW₁₁ was incorporated in the polyester film. The ratio of the relative intensity between the $^5D_0 \rightarrow ^7F_2$ transition and $^5D_0 \rightarrow ^7F_1$ transition was 1.8 in the EuSiW₁₁/polyester film and lower (1.12) in the EuSiW₁₁ solid. The $^5D_0 \rightarrow ^7F_2$ transition was considered hypersensitive to the site symmetry of Eu³⁺ ion; as a result, the increase of the ratio of the relative intensity of $^5D_0 \rightarrow ^7F_2$ / $^5D_0 \rightarrow ^7F_1$ suggested the lower symmetry of Eu³⁺ ion in the EuSiW₁₁/polyester film. The distortion of the symmetry may be due to the interaction between the polyester matrix and europium-substituted heteropolytungstates and resulting alteration of the transition energy levels of Eu³⁺.

3.3. Emission spectra of EuGeW₁₁/polyester film and EuGeW₁₁ solid

Fig. 6 depicts the emission spectra of the EuGeW₁₁ solid (solid line) and the EuGeW₁₁/polyester film (dash line). The characteristic emission peaks of Eu³⁺, which correspond to $^5D_0 \rightarrow ^7F_j$ ($j = 0-4$) transitions, can be observed both in the EuGeW₁₁ solid and in the EuGeW₁₁/polyester film.

Nevertheless, obvious differences can be observed in the emission spectrum of the EuGeW₁₁/polyester film as compared to that of the EuGeW₁₁ solid. In the emission spectrum of the EuGeW₁₁ solid, the most intense emissions $^5D_0 \rightarrow ^7F_1$ and $^5D_0 \rightarrow ^7F_2$ both split into two peaks. However, there is no splitting in the transition of $^5D_0 \rightarrow ^7F_1$ and $^5D_0 \rightarrow ^7F_2$ in the EuGeW₁₁/polyester film. The ratio of the relative intensity between $^5D_0 \rightarrow ^7F_2$ and $^5D_0 \rightarrow ^7F_1$ transition is higher in the EuGeW₁₁/polyester film than

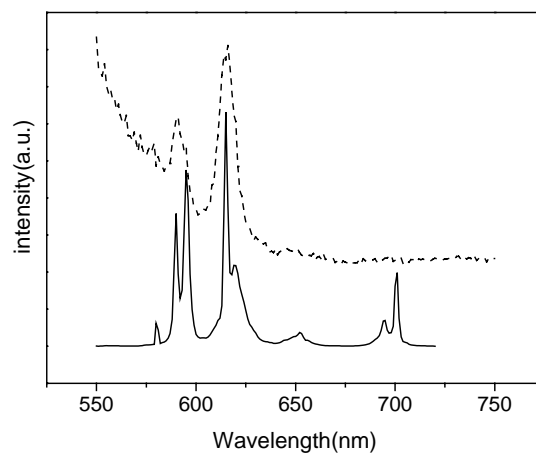


Fig. 6. Emission spectra of the EuGeW₁₁ solid (solid line) and the EuGeW₁₁/polyester film (dash line).

in the EuGeW₁₁ solid. Such changes are caused by the change of the site symmetry of Eu³⁺, as have been explained in the emission spectra of the EuSiW₁₁ solid and the EuSiW₁₁/polyester film.

3.4. Emission spectra of EuBW₁₁/polyester film and EuBW₁₁ solid

The emission spectra of the EuBW₁₁ solid (solid line) and the EuBW₁₁/polyester film (dash line) are shown in Fig. 7. Both of them consist of the characteristic emission lines of Eu³⁺, which correspond to $^5D_0 \rightarrow ^7F_j$ ($j = 0-4$) transitions. However, there exist differences in the number, the position and the relative intensity of the emission peaks between the spectrum of the EuBW₁₁ solid and the EuBW₁₁/polyester film. The emissions of $^5D_0 \rightarrow ^7F_2$ and $^5D_0 \rightarrow ^7F_1$ are the most intense emissions in the spectrum of the EuBW₁₁ solid and the EuBW₁₁/polyester film. The $^5D_0 \rightarrow ^7F_2$ (614, 622 nm) and $^5D_0 \rightarrow ^7F_1$ (592, 595 nm) transitions are split into two peaks in the EuBW₁₁ solid. Nevertheless, they are not split in the EuBW₁₁/polyester film. Another prominent

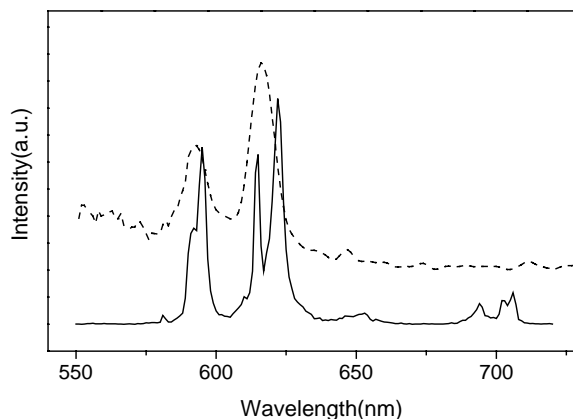


Fig. 7. Emission spectra of the EuBW₁₁ solid (solid line) and the EuBW₁₁/polyester film (dash line).

difference lies in the increase of the red to orange intensity ratio (R:O) of Eu^{3+} in the film as compared to the solid, which results from the lower site symmetry of Eu^{3+} in the EuBW_{11} /polyester film. In addition, there are fewer emissions in the spectrum of the EuBW_{11} /polyester film than in the EuBW_{11} solid, which can be explained by the ordered entrapment of EuBW_{11} in the EuBW_{11} /polyester film.

3.5. Lifetimes

The fluorescence decay curves of $^5\text{D}_0 \rightarrow ^7\text{F}_2$ emission for the EuSiW_{11} /polyester film and the EuSiW_{11} solid were measured. Both of the curves were single exponential. The lifetimes of Eu^{3+} were calculated to be 0.76 ms in the polyester film and 2.43 ms in the solid. It was obvious that Eu^{3+} showed shorter lifetime in the polyester film than in the solid, which may result from the intermolecular action between the polyester matrix and inorganic heteropolytungstates. The dimension of the materials may be another reason [13].

4. Conclusion

The hybrid organic/inorganic luminescent films have been successfully prepared by sol–gel method. LMCT band could be observed in the hybrid films, which could not be found in the solid. The films exhibit the characteristic emission bands of the rare earth ion. The emissions of $^5\text{D}_0 \rightarrow ^7\text{F}_2$ and $^5\text{D}_0 \rightarrow ^7\text{F}_1$ split in the solid but not in the polyester film. The ratio of the relative intensity between $^5\text{D}_0 \rightarrow ^7\text{F}_2$ and $^5\text{D}_0 \rightarrow ^7\text{F}_1$ transition increases after europium-substituted

heteropolytungstates are incorporated in the polyester film. The lifetime of Eu^{3+} is shorter in the polyester film than in the solid. These results can be ascribed to the intermolecular action between polyester matrix and heteropolytungstates and resulted distortion of the site symmetry of the Eu^{3+} ion in polyester films.

Acknowledgements

The authors are grateful to the Youth Foundation of Hubei University.

References

- [1] V. Bekiari, P. Lianos, *Adv. Mater.* 10 (1998) 1455.
- [2] G.E. Buono-core, H. Li, B. Marciniak, *Coord. Chem. Rev.* 99 (1990) 55.
- [3] J. Kido, H. Hayase, K. Hongawa, K. Nagai, *Appl. Phys. Lett.* 65 (1994) 2124.
- [4] L.R. Matthews, E.T. Knobbe, *Chem. Mater.* 5 (1993) 1697.
- [5] J. Wang, H. Wang, L. Fu, F. Liu, H. Zhang, *Thin Solid Films* 415 (2002) 242.
- [6] J. Wang, H. Wang, F. Liu, L. Fu, H. Zhang, *Mater. Lett.* 416 (2003) 1210.
- [7] X.L. Wang, Y.H. Wang, C.W. Hu, E.B. Wang, *Mater. Lett.* 56 (2002) 305.
- [8] N.K. Chaudhury, R. Bhardwaj, B.M. Murari, *Curr. Appl. Phys.* 3 (2003) 177.
- [9] R.D. Peacock, T.J.R. Weakley, *J. Chem. Soc. (A)* (1971) 1836.
- [10] S.A. Zubairi, S.M. Ifzal, A. Malik, *Inorg. Chim. Acta* 22 (1977) 29.
- [11] S. Lis, *J. Alloys Compd.* 300–301 (2000) 88.
- [12] G. Blasse, G.J. Dirksen, *J. Inorg. Nucl. Chem.* 43 (1981) 2847.
- [13] Y.L. Zhao, D.J. Zhou, G.Q. Yao, C.H. Huang, *Langmuir* 13 (1997) 4060.